

DETC2009-86364

MECHANICS OF HETEROGENEOUS FLUCTUATING ELASTIC RODS

Tianxiang Su

Mechanical Engineering and Applied Mechanics,
University of Pennsylvania,
Philadelphia, PA, 19104, USA.
Email: tsu@seas.upenn.edu.

Prashant K. Purohit*

Mechanical Engineering and Applied Mechanics,
University of Pennsylvania,
Philadelphia, PA 19104, USA.
Email: purohit@seas.upenn.edu.

ABSTRACT

Biofilaments, such as actin and DNA, have for long been modeled as thermally fluctuating elastic rods with homogeneous material properties. Such models are adequate if the length scale of the filaments being studied is much larger than the scale of the heterogeneity. However, advanced single molecule experimental techniques have now made it possible to probe the properties of biomolecules at the scale of a few nanometers. The data emerging from these experiments ought to be greeted with appropriately detailed models. In this paper we study the mechanics of a thermally fluctuating elastic rod whose moduli are a function of position. Such a rod can be used as a model for DNA whose sequence specific properties are known or for a protein oligomer in an AFM where some of the monomers might be unfolded. The mechanics of these rods is understood by first evaluating a partition function through path integral techniques. We develop a computational technique to efficiently evaluate the partition function and use it to obtain the force-extension relation of a fluctuating rod with two different bending moduli as would be the case for a partially unfolded protein oligomer stretched in an AFM. The variance of the transverse fluctuations of the protein oligomer is also evaluated and are found to agree with the results of a Monte Carlo simulation.

1 INTRODUCTION

Techniques for performing mechanical experiments on single molecules, such as, optical tweezers, magnetic tweezers and

the atomic force microscopes, have been refined over the last two decades. These techniques, which combine characteristics, such as, high force sensitivity, high positional accuracy and good compatibility with physiological environment, have been widely used to study molecule forces at the single-molecular level as well as structures of single bio-molecules [1–6]. The mechanical behavior of proteins, such as, actin, titin, ubiquitin etc., and those of nucleic acids, such as, single- and double-stranded DNA and RNA have been measured using these methods at length scales spanning a few tens of nanometers to a few microns. The measurements reveal that configurational entropy due to Brownian motion is a key player in the mechanics of these macromolecules.

Theoretically, it is generally acknowledged that a model of thermally fluctuating elastic rods is appropriate for describing the thermal and mechanical properties of rod-like biomolecules, such as, actin, DNA, etc. Other than taking the bending cooperativity into account, this model successfully captures their entropic elasticity and is widely used to interpret the experimental data on them [7–10]. The most well-known theory in this field is the worm-like chain (WLC) model dating back to the first half of the last century and gaining renewed interest in the last two decades [8,9]. Different properties of such fluctuating elastic rods, including the distribution of their end-to-end distance (extension), their force-extension relation under different boundary conditions, as well as their transverse fluctuations along the arc have been studied under the assumption that the mechanical properties are uniform [8–11]. However, recent experiments have been able to probe the properties of biomolecules at the scale of a few nanometers at which heterogeneity in the mechan-

*Address all correspondence to this author.

ical properties cannot be neglected. In fact, several recent studies have revealed the remarkable effects of the heterogeneous properties of some biopolymers on their conformations as well as their mechanical behaviors [12, 13]. For example, the protein projectin consists of domains that are significantly different in mechanical properties and shows distinct unfolding patterns even in a single pulling experiment [14]. The sequence dependence of the mechanical properties of DNA is suggested to be well sensed by DNA binding proteins and could be biologically significant [15–17]. Heterogeneous mechanical properties are also encountered in partially unfolded protein oligomers in atomic force microscopy [18]; protein unfolding has biologically significant implications in signalling [19]. As a final example, it has been noted that localized softening in DNA can have significant influence on looping probabilities [20] which ultimately affect regulation of genetic activity [21]. These examples show that heterogeneity in mechanical properties of biomolecules have significant biological consequences and motivate us to carefully examine the effects of heterogeneity via mathematical models.

Some earlier theoretical work on the WLC model can be modified to take heterogeneity into account [20], but theories on heterogeneous fluctuating elastic rods are rare in literature. A simple way of introducing heterogeneity in models of polymers is to group the monomers into H (hydrophobic) or P (hydrophilic) types as has been done in some recent articles [22–24]. The approach in this paper is different in that we study heterogeneous rods, whose bending modulus $K_b(s)$ is an arbitrary function of the arc length s , in a fixed force and fixed temperature ensemble using statistical mechanics. The partition function and free energy are evaluated first. The averages as well as the variances of the energy and the extension of the rod are calculated from the partition function. In particular, we show that the variance of the extension is just the slope of the extension-force profile scaled by the thermal energy. Also shown in the paper are the fluctuation of the tangential angles of the rod, as well as the variance of the transverse fluctuation. Monte Carlo simulations have been performed to verify our theoretical results.

2 PROBLEM DESCRIPTION

We begin with a statistical mechanical description of a N -segment fluctuating chain in this paper. The chain is a discrete version of a fluctuating elastic rod. As shown in Fig. 1, we define the direction of the end-to-end vector of the chain as the X -axis (the axis is fixed in the space and the end of chain is constrained to move on the axis). The segments of the chain are labeled 1 to N from one end to the other, and link i subtends an angle θ_i with respect to the X -axis. The preferred orientation of the segments of the chain is parallel to each other and there is a quadratic energy penalty associated with deviations from this configuration.

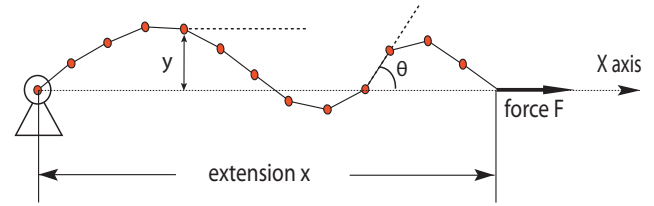


Figure 1. Model of the N -segment chain. The end-to-end vector of the chain defines the X axis along which an external force F is applied. The end-to-end distance of the chain (called extension) is x . Each link in the chain subtends an angle θ_i with the X axis and its transverse displacement from the axis is denoted as y_i .

Accordingly, the bending energy of the chain is given by:

$$E_b = \sum_{i=1}^N \frac{K_i}{2l} (\theta_{i+1} - \theta_i)^2, \quad (1)$$

where K_i is the bending modulus, which varies along the chain and l is the segment length. The chain considered here is assumed to be untwistable and inextensible, so that, elastic energy arises only from bending (Eq. (1)). The theory proposed here is for a 2D chain, but it is straightforward to generalize the results to a 3D untwistable and inextensible chain, provided that we use an appropriate set of angles to represent the chain [25]. Also, the authors note that twistable and extensible chains can be studied using the same theoretical framework as long as the elastic energy remains quadratic in the configuration angles θ_i .

The chain is in a heat bath at a fixed temperature T and is randomly bombarded by the small particles surrounding it. The segments of the chain are so small that the thermal energy and the bombardment are significant compared to the bending energy and cannot be ignored. In other words, the chain is fluctuating around its thermal equilibrium state.

Finally, a constant external force is exerted at one end of the chain while the other end is hinged (Fig. 1). We then ask questions, such as, what is the average end-to-end distance (denoted as extension below) of such a chain? What is the average bending energy? What is the magnitude of the fluctuations, i.e., what is the displacement of the chain from the X -axis and what is the variance of the extension and the energy? These questions are answered using the methods of thermodynamics.

3 THEORY

3.1 Fundamental Equation

Since both the temperature and force are fixed in our problem, the free energy G can be written as:

$$G(T, F) = E_b - TS - Fx, \quad (2)$$

which is an analogue of the Gibbs free energy with T and F being independent variables. S is the entropy. In such an ensemble, each configuration \mathbf{v} appears with probability [26]:

$$P_{\mathbf{v}} = \frac{1}{\exp(-\beta G)} \cdot \exp\left(-\frac{E_{b,\mathbf{v}} - Fx_{\mathbf{v}}}{k_B T}\right), \quad (3)$$

where $\beta = (k_B T)^{-1}$, k_B is the Boltzmann constant and x is the extension of the chain. The partition function is defined as

$$Z = \sum_{\mathbf{v}} \exp\left(-\frac{E_{b,\mathbf{v}} - Fx_{\mathbf{v}}}{k_B T}\right), \quad (4)$$

and is related to the free energy G as follows:

$$Z = \exp(-\beta G), \quad G = -k_B T \log Z, \quad (5)$$

which is due to the fact that $\sum_{\mathbf{v}} P_{\mathbf{v}} = 1$.

The partition function Z in Eq. (4) involves a sum over all configurations of the chain and becomes a path integral when the number of segments N becomes infinite and the segment length l goes to zero in such a way that their product Nl remains fixed. Zhang and Crothers [17] (see also [27]) have provided an efficient way to compute this partition sum. The result turns out to be simply a problem of evaluating the determinant of a $N + 1$ by $N + 1$ matrix in our case (under the assumption that θ_i are small). A glimpse of this calculation appears in section 3.4. Once the partition function is obtained, we can obtain all the thermodynamic quantities for the chain, as discussed below.

3.2 Average Extension and Its Variance

We are interested in the average value of the extension and also its variance under the constant applied force. To address this problem, we remember that

$$dE_b = T dS + F dx. \quad (6)$$

Using Eq. (2), we get,

$$dG = -SdT - x dF, \quad (7)$$

therefore,

$$x = -\left(\frac{\partial G}{\partial F}\right)_T = k_B T \left(\frac{\partial \log Z}{\partial F}\right)_T, \quad (8)$$

where we have used Eq. (5) to get the last result.

To evaluate the variance of x , we take the derivative of x with respect to the quantity which is conjugate to x in the entropy function $S(x, E_b)$ [26]. We note that

$$dS = -\frac{F}{T} dx + \frac{1}{T} dE_b, \quad (9)$$

and, therefore,

$$\langle \Delta x^2 \rangle = -k_B \left(\frac{\partial x}{\partial (-\frac{F}{T})}\right)_{\frac{1}{T}} = k_B T \left(\frac{\partial x}{\partial F}\right)_T. \quad (10)$$

Equation (10) shows that the fluctuation of extension is simply the slope of the extension-force relation scaled by the thermal energy $k_B T$ and further implies that $(\partial x / \partial F)_T$ is always non-negative, which is in accordance with our intuition. Equation (10) does not imply, however, that the fluctuation scales linearly with temperature T because the derivative on the right-hand-side itself is a function of the temperature. In fact, using the force-extension relation for a homogeneous worm-like chain [11], one finds that the slope of the extension-force profile depends linearly on T , and therefore the fluctuation $\langle \Delta x^2 \rangle$ scales as T^2 .

3.3 Average Energy and Its Variance

From the definition of the partition function (Eq. (4)), one can easily show that the average bending energy is given by:

$$\langle E_b \rangle = -\left(\frac{\partial \log Z}{\partial \beta}\right)_F + F \langle x \rangle, \quad (11)$$

where $\langle x \rangle$ is obtained in the previous subsection (Eq. (8)). The variance of bending energy is related to the derivative of E_b with respect to β at fixed ratio of F and T [26], and is given by:

$$\langle \Delta E_b^2 \rangle = -k_B \left(\frac{\partial E_b}{\partial (\frac{1}{T})}\right)_{F/T} = k_B T^2 \left(\frac{\partial E_b}{\partial T}\right)_{F/T}. \quad (12)$$

We note that the quantity $\left(\frac{\partial E_b}{\partial T}\right)_{F/T}$ is not the heat capacity C_V or C_P we are familiar with since it is evaluated at fixed F/T .

Equation (12) is not convenient for computation since its independent variables are $1/T$ and F/T . By changing variables to F and T , we obtain:

$$\langle \Delta E_b^2 \rangle = k_B T \left[T \left(\frac{\partial E_b}{\partial T} \right)_F + F \left(\frac{\partial E_b}{\partial F} \right)_T \right], \quad (13)$$

which is more useful for a fixed T, F ensemble. If we further change the variables to x and S , we can express the fluctuation in terms of the three material properties – heat capacity at constant F , thermal expansion coefficient and isothermal extensibility:

$$\langle \Delta E_b^2 \rangle = k_B T^2 \cdot \left[T \left(\frac{\partial S}{\partial T} \right)_F \right] + 2k_B T^2 \cdot F \cdot \left[\left(\frac{\partial x}{\partial T} \right)_F \right] \quad (14)$$

$$+ k_B F^2 T \left[\left(\frac{\partial x}{\partial F} \right)_T \right]. \quad (15)$$

3.4 Equipartition theorem in a fixed T, F ensemble

The equipartition theorem provides us another way of analyzing the energy, and it is also a criterion used in simulations to determine whether equilibrium has been reached.

We first rewrite the partition function (Eq. (4)) as:

$$Z = \exp(\beta FL) \int_{-\pi}^{+\pi} \cdots \int_{-\pi}^{+\pi} \exp[-\beta(E_b - Fx + FL)] d\vec{\theta}. \quad (16)$$

Here, $\vec{\theta} = [\theta_1, \theta_2, \dots, \theta_d]^T$ and d is the number of independent segment angles in the chain. Note that d depends on the boundary conditions, which in general, will pose a number of constraints on the segment angles. The term $(E_b - Fx + FL)$ reaches its minimum 0 when $\theta_i \equiv 0$. Therefore, we rewrite it in a quadratic form $(\vec{\theta}^T \mathbf{M}^* \vec{\theta})$ and apply the Laplace method [28] to Eq. (16) to get:

$$Z = \exp(\beta FL) \int_{-\infty}^{+\infty} \cdots \int_{-\infty}^{+\infty} \exp[-\beta(\vec{\theta}^T \mathbf{M}^* \vec{\theta})] d\vec{\theta}. \quad (17)$$

The matrix \mathbf{M} is positive definite and symmetric; so we can diagonalize it and Eq. (17) now reads:

$$Z = e^{\beta FL} \left(\int_{-\infty}^{+\infty} \exp(-\beta \rho_1^2 \Lambda_1) d\rho_1 \right) \cdots \left(\int_{-\infty}^{+\infty} \exp(-\beta \rho_d^2 \Lambda_d) d\rho_d \right), \quad (18)$$

where $\Lambda = \text{diag}[\Lambda_1, \dots, \Lambda_d]$ is the diagonalized matrix and the independent variables have changed to ρ_i . If we denote

$$Z_i = \int_{-\infty}^{+\infty} \exp(-\beta \rho_i^2 \Lambda_i) d\rho_i = \sqrt{\frac{\pi}{\beta \Lambda_i}}, \quad (19)$$

then

$$\langle \rho_i^2 \Lambda_i \rangle = \frac{\int_{-\infty}^{+\infty} \Lambda_i \rho_i^2 \exp(-\beta \Lambda_i \rho_i^2) d\rho_i}{\int_{-\infty}^{+\infty} \exp(-\beta \Lambda_i \rho_i^2) d\rho_i} = -\frac{\partial \log Z_i}{\partial \beta} = \frac{1}{2\beta} = \frac{1}{2} k_B T. \quad (20)$$

Finally, we arrive at:

$$\langle E_b \rangle - F \langle x \rangle + FL = \langle \vec{\theta}^T \mathbf{M}^* \vec{\theta} \rangle = \sum_{i=1}^d \langle \rho_i^2 \Lambda_i \rangle = \frac{d}{2} k_B T. \quad (21)$$

We note that for an ensemble in which T and F are fixed, it is not the average energy E_b , but instead, $\langle E_b \rangle - F \langle x \rangle + FL$ that is equipartitioned.

3.5 Transverse Fluctuation of The Chain

The transverse fluctuation of a homogeneous chain under different boundary conditions has been discussed in detail by Purohit *et al.* [11]. In general, for a heterogeneous chain, this fluctuation is given by:

$$\langle y_k^2 \rangle = \left\langle \left(\sum_{i=1}^k l \sin \theta_i \right)^2 \right\rangle \approx l^2 \sum_{i,j=1}^k \langle \theta_i \cdot \theta_j \rangle, \quad (22)$$

where

$$\langle \theta_i \cdot \theta_j \rangle = \frac{1}{Z} \int_{-\pi}^{+\pi} \cdots \int_{-\pi}^{+\pi} (\theta_i \cdot \theta_j) \exp[-\beta(E - Fx)] d\vec{\theta}. \quad (23)$$

Note that such a quantity can be computed analytically (see [17] for details), and thus the variance of the transverse deflections can be computed.

4 MONTE CARLO SIMULATION

To verify the theoretical results stated above, we performed MC simulations for four 250-segment heterogeneous chains (segment length 0.1nm) with hinged-hinged boundary conditions on the two ends. The four chains (we call them chain 1 to 4 below) differ from each other in their bending moduli as a function of position along the chain. Chain 1 has a uniform bending modulus of $2.0k_B T \cdot \text{nm}$; chain 2 has a bending modulus of $2.0k_B T \cdot \text{nm}$ for the first 75 segments and $0.4k_B T \cdot \text{nm}$ for the rest of the segments. This chain has only two bending moduli and we call it a special heterogeneous chain in the discussion below. Chain 3 has a bending modulus that is linearly increasing with the segment number i , with an average value of $2.0k_B T \cdot \text{nm}$ and highest value of $3.5k_B T \cdot \text{nm}$. Finally, the bending modulus of chain 4

is a sine function along the chain, with the maximum and minimum values being $3.5k_B T \cdot \text{nm}$ and $0.5k_B T \cdot \text{nm}$ respectively. Of these, chain 1 and chain 2 are relevant to real biomolecules, such as, DNA and proteins. Chain 3 and chain 4 are both theoretical constructs. However, we note that chain 4 could be relevant since any function $K(s)$ (the s dependent bending modulus, in this case) on the domain $0 \leq s \leq L$ can be approximated by a Fourier series and chain 4 will then represent one term of such a series.

For all the discussions related to the simulations below (except for the force-extension profile in which the force is changing), a fixed force of 1000pN is applied at the end of the chain along the direction of the end-to-end vector. The end-to-end distance of the chain is free to fluctuate and the temperature is set to 300K for all the simulations.

In accordance with the theory, the configuration of chain is characterized by N segment angles θ_i . New conformations of the chain are generated from the existing one by randomly varying $N/2$ of the existing angles. The new conformation is accepted with a probability according to the Metropolis criterion [29], and the equipartition theorem (Eq. (21)) is applied to check whether the chain is in equilibrium.

5 RESULTS

Fig. 2 shows the energy E_b (blue) as well as $E_b - Fx + FL$ (black) in the process of the MC simulation for chain 4 (the results for chain 1-3 are very similar and are not shown). The red line in the figure is the equipartition value $(N/2)k_B T$, whereas the red dashed and red dot-dashed lines are the theoretical predictions for $\langle E_b \rangle$ and $\langle E_b \rangle \pm \sqrt{\langle \Delta E^2 \rangle}$ (Eq. (11) and Eq. (13)). The MC simulation result confirms that it is $E_b - Fx + FL$, rather than the energy E_b itself, being equipartitioned. In addition, the theory and the MC simulation show good agreement for the average energy (261.2 pN·nm versus 260.7 pN·nm) and its standard deviation (26.5 pN·nm versus 26.6 pN·nm). We note that since the equipartition theorem is satisfied and the system has reached equilibrium, the analysis and the comparisons with the theoretical results in the following discussions are valid. Fig. 3 shows the theoretical and MC simulation results for the relative extension x/L and its standard deviation (L is the contour length of the chain). Fig. 3A is for the special heterogeneous chain (chain 2) and Fig. 3B is for the chain with linearly increasing bending modulus (chain 3). This figure shows that our theory correctly predicts the average value and variance of the extension for the heterogeneous chains (for detailed data, see the caption of Fig. 3). In fact, our prediction shows that the standard deviation for chain 2 is slightly larger than that of chain 3 and this is confirmed by the simulation results.

To obtain the full force-extension relation, we varied the force in the MC simulation to obtain the average extension under different forces. The result for chain 4, whose bending modulus

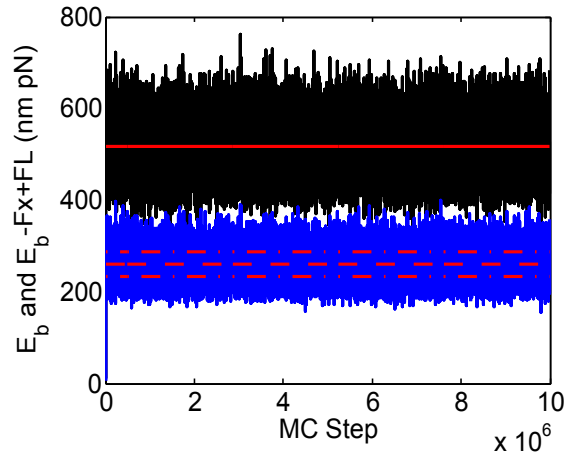


Figure 2. Energy E_b (blue), $E_b - Fx + FL$ (black), equipartition value $(N/2)k_B T$ (red) and theoretical prediction for the energy (red dashed line) as well as its standard deviation (red dot-dashed lines) throughout the MC simulation for a chain along which the bending modulus is a sine function (chain 4). It is clear that it is not the energy itself being equipartitioned. This figure also shows a good match between our theoretical prediction for the energy and the MC simulation results.

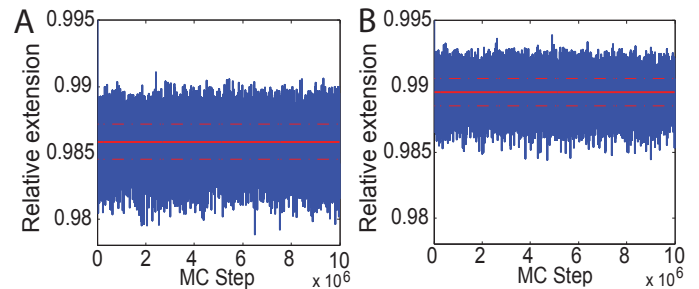


Figure 3. Relative extension for chain 2 (A) and chain 3 (B). Data collected from the MC simulation is shown in blue. The red lines are the theoretical predictions for the average extension (Eq. (8)). The distance between the red dot-dashed line and the red line is the theoretical prediction for the standard deviation (Eq. (10)). For chain 2, the theoretical analysis and MC simulation show exactly the same result: $\langle x/L \rangle = 0.986$, $\sigma = 1.3 \times 10^{-3}$. For chain 3, the theory and simulation again give the same result for the average: $\langle x/L \rangle = 0.990$, while the theoretical calculation shows $\sigma = 1.1 \times 10^{-3}$ and the simulation shows $\sigma = 1.0 \times 10^{-3}$.

is changing periodically, is shown as red circles in Fig. 4. In comparison, we plot our theoretical result (Eq. (8)) as a black curve in the same figure. The figure shows that the theoretical and the simulation results match with each other quite well. The $\langle \theta_i^2 \rangle$ profile is plotted in Fig. 5A, B, C and D for chain 1-4 respectively. The red circles are the MC simulation results, which agree

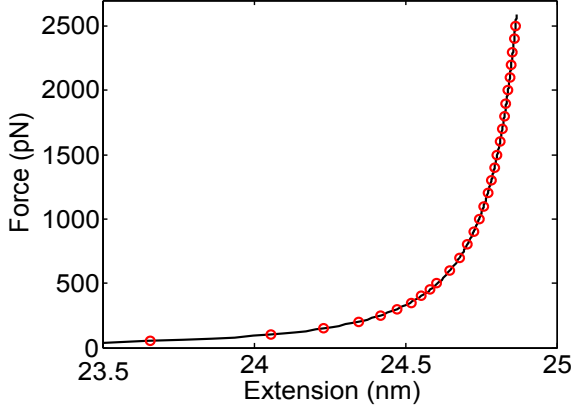


Figure 4. Force-extension relation for chain 4. We try forces ranging from 50pN to 2500pN in the MC simulations and obtain the corresponding average extension under these forces (red circles). In comparison, we plot our theoretical prediction (Eq. (8)) as the black curve in the figure, which as shown, passes through all the red circles.

with the theoretical predictions (black, Eq. (23)) for all the four cases. When the chain is homogeneous, the $\langle \theta_i^2 \rangle$ profile is almost flat in the middle of the chain, while if there is a jump in the bending modulus in the chain, as in chain 2, the $\langle \theta_i^2 \rangle$ profile shows a corresponding discontinuity. For chain 2, the bending modulus is larger in the first part of the chain, so it is expected that $\langle \theta_i^2 \rangle$ will be smaller. For chain 3, whose bending modulus increases linearly, the $\langle \theta_i^2 \rangle$ profile does not decrease linearly, but in a manner shown in Fig. 5C. Finally, the $\langle \theta_i^2 \rangle$ profile for chain 4 varies periodically in accordance with its change in bending modulus as shown in Fig. 5D. We have also calculated the variance of the transverse displacement and the results are shown in Fig. 6A, B, C and D, for chain 1-4 respectively. Interestingly, both simulation and theoretical calculation show that the four profiles look similar, meaning that the transverse displacement is not sensitive to the distribution of bending modulus at high forces.

6 DISCUSSION AND CONCLUSION

The theory proposed in the paper is able to reproduce the results of the Monte Carlo simulations: but, it is important to ask how this depends on the parameters we have chosen. There are three independent free parameters in our theory: the bending modulus K_b (can be a function of the arc length s), segment length l and contour length L . To reduce the number of parameters, one can let $l \rightarrow 0$ (with $N \rightarrow +\infty$, keeping $L = Nl$ fixed), so that the chain becomes a continuous rod and has only two parameters K_b and L that have clear corresponding physical meanings for biopolymers. The question is how fast the results discussed in this paper converge as $l \rightarrow 0$, or how small should l be, in order

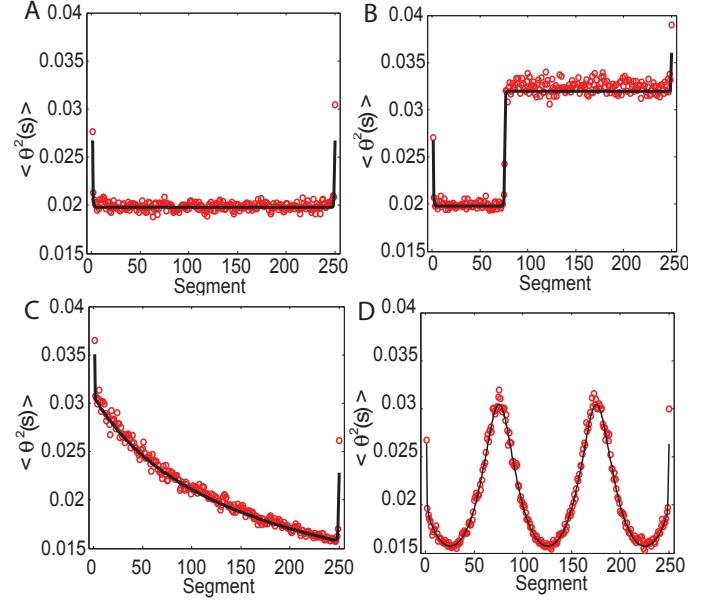


Figure 5. $\langle \theta_i^2 \rangle$ versus i , the segment number. Red circles: MC simulation results, red: theoretical prediction using Eq. (23). A, B, C, D are for a homogeneous chain, a special heterogeneous chain with only two bending moduli, a chain with linearly increasing bending modulus and a chain with sinusoidally varying bending modulus respectively.

that the chain be viewed as a continuous rod?

To address this problem, we try several different segment lengths l and see how the following quantities converge as l approaches zero: (1) the force-extension profile, (2) the variance of the extension under a constant force, (3) the fluctuation in the angle θ_i , and (4) the transverse fluctuation of the chain. The parameters and the results are shown in Table. 1 and Fig. 7. For simplicity, we discuss homogeneous chains here. Table. 1 shows the average extensions for different choices of l under a constant force of 500pN. To see how the result converges, we also consider the limit case as l approaches 0 with $L = Nl$ fixed. In this limit, the homogeneous discrete chain becomes a continuous rod and we use the following formula to compute its average extension [11]:

$$x = L - \frac{k_B T}{4} \left[\frac{L}{\sqrt{K_b F}} \coth \left(L \frac{F}{K_b} \right) - \frac{1}{F} \right]. \quad (24)$$

The table shows that smaller segment length l leads to smaller average extension $\langle x \rangle$, reflecting that the chain is more flexible, which is expected. All the relative errors (with respect to the average extension of the continuous rod) remain below 1% in the cases studied. Fig. 7 plots the average extension, variance in extension, as well as the fluctuation for the chains listed in Table. 1. All the results show that a chain with $\xi_p/l \gtrsim 100$ can

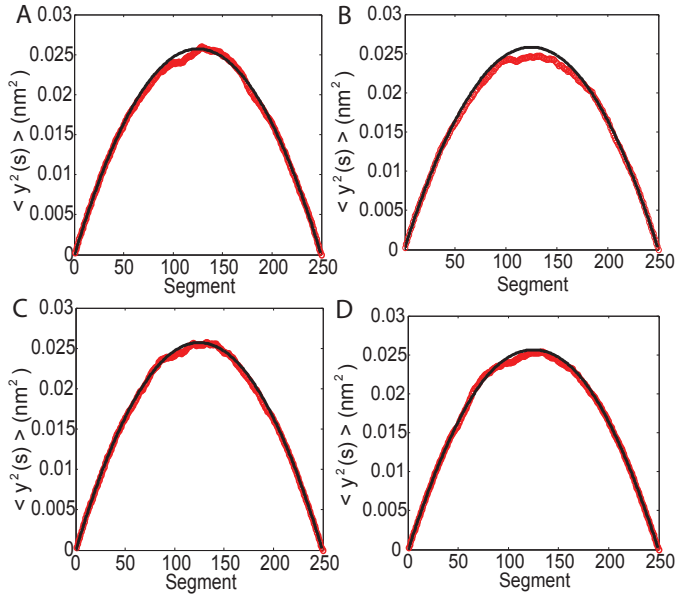


Figure 6. $\langle y_i^2 \rangle$ versus i , the segment number. Red: MC simulation results, black: theoretical predictions using Eq. (22). Figure A, B, C, and D are for a homogeneous chain, a special heterogeneous chain with only two bending moduli, a chain with linearly increasing bending modulus and a chain whose bending modulus is a sine function respectively.

well represent a continuous rod (results converged). In particular, for the transverse fluctuation, the results for all the chains, with ξ_p/l ranging from 8 to 800, almost coincide. It should be noted that although the chain can be viewed as a continuous rod only when l is chosen to be small, the theory proposed in this paper is valid regardless how small l is compared with ξ_p .

In conclusion, we have developed a computational technique to study the thermomechanics of a heterogeneous fluctuating elastic rod. We first compute a partition function for the corresponding statistical mechanical problem and use it to calculate quantities such as the free energy, the average extension, variance of transverse displacements, etc. We also compare our results with those of Monte Carlo simulations and find excellent agreement. The chief advantage of our computational method is its speed and its ability to easily account for heterogeneity as well as a variety of boundary conditions. In some cases, such as, the special heterogeneous chain with only two bending moduli, it is possible to derive analytical expressions from our theory that can be fit to data from AFM experiments on protein oligomers. In a subsequent publication we will show how to use our heterogeneous fluctuating rod model to interpret such experiments.

Table 1. Parameters of the chains and average extensions of the chains under a fixed force of 500pN. Temperature T , bending modulus K_b and contour length L are the same for all the chains. N is the number of segments in the chain, l is the segment length, ξ_p is the persistence length for the 2D chain. The results show that chains with larger segment lengths are less flexible because they have larger average extensions. The error is computed relative to the average extension of the corresponding continuous rod in the third row (Eq. (24)). It remains under 1% for all the chains studied.

$T = 300 \text{ K}, \xi_p = 4.0 \text{ nm (2D chain)}, L = 25 \text{ nm}, F = 500 \text{ pN}$				
N	l (nm)	ξ_p/l	$\langle x \rangle$ in nm	Relative Error %
$+\infty$	0	$+\infty$	24.5999	0
5000	0.005	800	24.6000	0.0004
2500	0.01	400	24.6002	0.0012
500	0.05	80	24.6074	0.0305
250	0.1	40	24.6275	0.1122
125	0.2	20	24.6852	0.3472
100	0.25	16	24.7146	0.4663
50	0.5	8	24.8197	0.8935

REFERENCES

- [1] Lee, C.K., Wang, Y.M., Huang, L.S. and Lin, S., 2007, "Atomic Force Microscopy: Determination of Unbinding Force, Off Rate and Energy Barrier for Protein-Ligand Interaction," *Micron*, **38**(5), pp. 446-461.
- [2] Zhuang, X. and Rief, M., 2003, "Single-Molecule Folding," *Current Opinion in Structural Biology*, **13**(1), pp. 88-97.
- [3] Kellermayer, M.S., Smith, S.B., Granzier, H.L. and Bustamante, C., 1997, "Folding-Unfolding Transitions in Single Titin Molecules Characterized with Laser Tweezers," *Science*, **276**(5315), pp. 1112-1116.
- [4] Tskhovrebova, L., Trinick, J., Sleep, J.A. and Simmons, R.M., 1997, "Elasticity and Unfolding of Single Molecules of the Giant Muscle Protein Titin," *Nature*, **387**(6630), pp. 308-312.
- [5] Liphardt, J., Onoa, B., Smith, S.B., Tinoco, I., JR. and Bustamante, C., 2001, "Reversible Unfolding of Single RNA Molecules by Mechanical Force," *Science*, **292**(5517), pp. 733-737.
- [6] Rief, M., Gautel, M., Oesterhelt, F., Fernandez, J.M. and Gaub, H.E., 1997, "Reversible Unfolding of Individual Titin Immunoglobulin Domains by AFM," *Science*, **276**(5315), pp. 1109-1112.
- [7] Bustamante, C., Marko, J.F., Siggia, E.D. and Smith, S.,

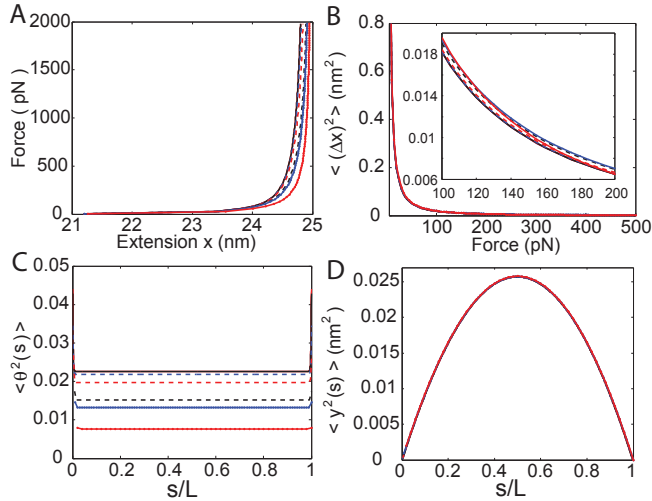


Figure 7. Blue: continuous rod; red and black solid lines ($N = 5000$, 2500 respectively), blue, red, black dashed lines ($N = 500$, 250, 125 respectively), blue and red dotted lines ($N = 100$, 50 respectively): The corresponding ξ_p/l values for the discrete chains are 800, 400, 80, 40, 20, 16, 8 respectively. Other parameters are listed in Table.1. (A) average extension of the chains; (B) variance of the extension (inset: an enlarged view); (C) fluctuation of the angle θ_i ; (D) transverse fluctuation of the chain.

1994, "Entropic Elasticity of Lambda Phage DNA," *Science*, **265**(5178), pp.1599-1600.

[8] Marko, J.F. and Siggia, E.D., 1995, "Stretching DNA," *Macromolecules*, **28**(26), pp. 8759-8770.

[9] Odijk, T., 1995, "Stiff Chains and Filaments under Tension," *Macromolecules*, **28**(20), pp. 7016-7018.

[10] Nelson, P., 2008, *Biological Physics: Energy, Information, Life*, W. H. Freeman and Company, New York.

[11] Purohit, P.K., Arsenault, M.E., Goldman, Y. and Bau, H.H., 2008, "The Mechanics of Short Rod-like Molecules in Tension," *International Journal of Non-Linear Mechanics*, **43**(10), pp. 1056-1063.

[12] Popov, Y.O. and Tkachenko, A.V., 2007, "Effects of Sequence Disorder on DNA Looping and Cyclization," *Physical Review E*, **76**(2 Pt 1), 021901.

[13] Moukhtar, J., Fontaine, E., Faivre-Moskalenko, C. and Arneodo, A., 2007, "Probing Persistence in DNA Curvature Properties with Atomic Force Microscopy," *Physical Review Letters*, **98**(17), 178101.

[14] Bullard, B., Garcia, T., Benes, V., Leake, M.C., Linke, W.A. and Oberhauser, A.F., 2006, "The Molecular Elasticity of the Insect Flight Muscle Proteins Projectin and Kettin," *Proceedings of the National Academy of Sciences of the United States of America*, **103**(12), pp. 4451-4456.

[15] Hogan, M., Legrange, J. and Austin, B., 1983, "Depen-

dence of DNA Helix Flexibility on Base Composition," *Nature*, **304**(5928), pp. 752-754.

[16] Hagerman, P.J., 1988, "Flexibility of DNA," *Annual Review of Biophysics and Biophysical Chemistry*, **17**, pp. 265-286.

[17] Zhang, Y. and Crothers, D.M., 2003, "Statistical Mechanics of Sequence-Dependent Circular DNA and Its Application for DNA Cyclization," *Biophysical Journal*, **84**(1), pp. 136-153.

[18] Su, T. and Purohit, P.K., 2009, "Mechanics of Forced Unfolding of Proteins," *Acta Biomaterialia*, In Press, DOI: 10.1016/j.actbio.2009.01.038.

[19] Sawada, Y., Tamada, M., Dubin-Thaler, B.J., Cherniavskaya, O., Sakai, R., Tanaka, S. and Sheetz, M.P., 2006, "Force Sensing by Mechanical Extension of the Src Family Kinase Substrate p130Cas," *Cell*, **127**(5), pp. 1015-1026.

[20] Wilson, D.P., Lillian, T., Goyal, S., Tkachenko, A.V., Perkins, N.C. and Meiners, J., 2007, "Understanding the Role of Thermal Fluctuations in DNA Looping," *Proceeding of SPIE*, **6602**, 660208.

[21] Purohit, P.K. and Nelson, P.C., 2006, "Effect of Supercoiling on Formation of Protein-Mediated DNA Loops," *Physical Review E*, **74**(6 Pt 1), 061907, pp. 1-14.

[22] Jarkova, E., Vlugt, T.J. and Lee, N.K., 2005, "Stretching a Heteropolymer," *The Journal of Chemical Physics*, **122**(11), 114904.

[23] Geissler, P.L. and Shakhnovich, E.I., 2002, "Reversible Stretching of Random Heteropolymers," *Physical Review E*, **65**(5 Pt 2), 056110.

[24] Jarkova, E., Lee, N.K. and Obukhov, S., 2005, "Extracting Structural Information of a Heteropolymer from Force-Extension Curves," *Macromolecules*, **38**(6), pp. 2469-2474.

[25] Kulić, I., 2004, "Statistical Mechanics of Protein Complexed and Condensed DNA," Thesis, Max Planck Institute for Polymer Research, Mainz, Germany.

[26] Callen, H.B., 1985, *Thermodynamics and an Introduction to Thermostatistics*, John Wiley and Sons, New York, Chichester, Brisbane, Toronto, Singapore.

[27] Su, T., 2008, "A Model for Forced Unfolding of Proteins," Technical Report, Department of Mechanical Engineering and Applied Mechanics, University of Pennsylvania, pp. 1-30.

[28] Carrier, G.F., Krook, M. and Pearson, C.E., 2005, *Functions of a Complex Variable: Theory and Technique*, Society for Industrial and Applied Mathematics, Philadelphia.

[29] Allen, M.P. and Tildesley, D.J., 1987, *Computer Simulation of Liquids*, Oxford Science, Oxford.